TTP09-18
SFB/CPP-09-51
arXiv:0907.2117

Low energy moments of heavy quark current correlators at four loops

A. Maier [a], P. Maierhöfer [a], P. Marquard [a] and A. V. Smirnov [b]

[a] *Institut für Theoretische Teilchenphysik, Universität Karlsruhe, Karlsruhe Institute of Technology (KIT), 76128 Karlsruhe, Germany*

[b] *Scientific Research Computing Center of Moscow State University, Russia*

Abstract

We describe several techniques for the calculation of multi-loop integrals and their application to heavy quark current correlators. As new results, we present the four-loop correction to the second and third physical moment in the low-energy expansions of vector, axial-vector and scalar quark current correlators. Using a Ward identity, we obtain the third and fourth moment for the pseudo-scalar correlator. We briefly discuss the impact of these results on the determination of the charm quark mass and the strong coupling constant using lattice simulations for the current correlators and of the charm- and bottom-quark mass from experimental data for $\sigma(e^+e^- \to \text{hadrons})$.

Key words: Perturbative calculations, Quantum Chromodynamics, Dispersion Relations, Heavy Quarks
PACS: 12.38.Bx, 12.38.-t, 11.55.Fv, 14.65.Dw, 14.65.Fy

1 Introduction

One of the phenomenologically most interesting applications of heavy quark current correlators is the determination of fundamental parameters of QCD via sum rules. Low-energy moments of the vector correlator can be compared to weighted integrals over the experimentally measured R-ratio, $R(s) = \sigma(e^+e^- \to \text{hadrons})/\sigma(e^+e^- \to \mu^+\mu^-)$, to determine values for the charm- and bottom-quark masses [1–4]. Recently "data" from lattice simulations have been used instead of experimental results and indeed this method has become a competitive way of extracting the charm-quark mass and the strong coupling

constant [5]. Although the correlators of all four (axial-vector, vector, scalar and pseudo-scalar) currents can be used in the lattice method, the most accurate predictions presented in [5] were based on the pseudo-scalar correlator.

In order to obtain precise values for the quark masses, it is mandatory to calculate higher order QCD corrections. To match the experimental precision this means calculations in four-loop approximation have to be performed. Improvements in both computer power and the techniques of multi-loop calculations have lead to significant progress in recent years.

After the second moment at order α_s^3 of the vector current became available it was possible to construct a Padé approximant of the vacuum polarization function [6]. This also leads to a prediction for the higher moments. With the explicit calculation of the third moment this prediction can be checked and it becomes possible to further improve the Padé approximation [7].

The three-loop, i.e. $\mathcal{O}(\alpha_s^2)$, corrections were evaluated more than ten years ago in [8–10] for vector, axial-vector, scalar and pseudo-scalar currents in the low energy expansion up to $(q^2)^8$. This calculation has employed the reduction method proposed in [11]. Recently, a different approach based on the combination of the Laporta algorithm [12] with differential equations [13–15] was used to calculate these corrections for terms up to $(q^2)^{30}$ [16,17].

At four-loop order, for the vector correlator the first physical moment proportional to $(q^2)^1$ was obtained in [18,19]. The second moment of this correlator was presented in [20], where, aside from the Laporta algorithm, also techniques based on Sbases and special treatment of internal self-energies were used for checks. These methods will be explained in detail in the paper at hand. Using the method mentioned in the previous paragraph, the thirty lowest moments of the double-fermionic corrections at $\mathcal{O}(\alpha_s^3 n_f^2)$ were determined in [21]. The part proportional to $\mathcal{O}(\alpha_s^n n_l^{(n-1)})$ is even known to all orders in perturbation theory [22].

For the pseudo-scalar correlator, the first moment and second moment at $\mathcal{O}(\alpha_s^3)$ are given in [23], together with the first moment of the axial-vector and the scalar correlator.

In this work, we present the calculation of the second and third moments of the vector, axial-vector and scalar correlators and the third and fourth moments of the pseudo-scalar correlator. In Section 2 we define our notation and explain the methods used in the calculation. In Section 3 we present a newly developed method for the efficient treatment of diagrams containing self-energy insertions. Section 4 contains the results for the various currents and an update of the determination of charm- and bottom-quark masses from experimental data and α_s from lattice calculations is given in Section 5. We

conclude in Section 6.

2 Methods

The polarization functions are defined by

$$(-q^2 g_{\mu\nu} + q_\mu q_\nu)\Pi^\delta(q^2) + q_\mu q_\nu \Pi_L^\delta(q^2) = i \int dx e^{iqx} \langle 0|T j_\mu^\delta(x) j_\nu^\delta(0)|0\rangle \quad (1)$$

$$\text{for} \quad \delta = v, a,$$

$$q^2 \Pi^\delta(q^2) = i \int dx e^{iqx} \langle 0|T j^\delta(x) j^\delta(0)|0\rangle \quad (2)$$

$$\text{for} \quad \delta = s, p,$$

with the currents

$$j_\mu^v = \bar{\psi}\gamma_\mu\psi, \quad j_\mu^a = \bar{\psi}\gamma_\mu\gamma_5\psi, \quad j^s = \bar{\psi}\psi, \quad j^p = i\bar{\psi}\gamma_5\psi. \quad (3)$$

In the low energy limit each of the polarization functions can be written as a series in $z = \frac{q^2}{4m^2}$, where m is the mass of the heavy quark and Q_q the corresponding charge,

$$\Pi^\delta(q^2) = \frac{3Q_q^2}{16\pi^2} \sum_{n>0} C_n^\delta z^n. \quad (4)$$

The coefficients C_n^δ can be expanded in a power series in $\frac{\alpha_s}{\pi}$:

$$C_n^\delta = C_n^{(0),\delta} + \frac{\alpha_s}{\pi} C_F C_n^{(1),\delta} + \left(\frac{\alpha_s}{\pi}\right)^2 C_n^{(2),\delta} + \left(\frac{\alpha_s}{\pi}\right)^3 C_n^{(3),\delta} + \cdots . \quad (5)$$

The decomposition of the four-loop contribution $C_n^{(3),\delta}$ according to the number of internal quark loops and its colour structure leads to

$$\begin{aligned} C_n^{(3),\delta} = {} & C_F T_F^2 n_l^2 C_{ll,n}^{(3),\delta} + C_F T_F^2 n_h^2 C_{hh,n}^{(3),\delta} + C_F T_F^2 n_l n_h C_{lh,n}^{(3),\delta} + C_{n_f^0,n}^{(3),\delta} \\ & + C_F T_F n_l \left(C_A C_{lNA,n}^{(3),\delta} + C_F C_{lA,n}^{(3),\delta}\right) + C_F T_F n_h \left(C_A C_{hNA,n}^{(3),\delta} + C_F C_{hA,n}^{(3),\delta}\right) . \end{aligned} \quad (6)$$

Here $C_F = \frac{N_C^2-1}{2N_C}$ and $C_A = N_C$ are the Casimir operators of the fundamental and adjoint representation of the $SU(N_C)$ group, respectively. $T_F = \frac{1}{2}$ is the index of the fundamental representation. n_h and n_l denote the number of heavy and light quarks, respectively. $C_{n_f^0,n}^{(3),\delta}$ contains the purely bosonic contributions, where we set the number of colours $N_C = 3$ for simplicity.

As described in [4] the theoretically computed moments C_n can be combined with measurements of the cross section of $e^+e^- \to$ hadrons to determine the

masses of charm and bottom quarks. The method is based on the dispersion relation

$$\Pi(q^2) = \frac{1}{12\pi^2} \int_0^\infty ds \frac{R(s)}{s(s-q^2)}\,, \tag{7}$$

where

$$R(s) = \frac{\sigma(e^+e^- \to \text{hadrons})}{\sigma(e^+e^- \to \mu^+\mu^-)}\,. \tag{8}$$

Taylor expanding both sides of Eq. (7) leads to

$$m = \frac{1}{2}\left(\frac{9Q_q^2}{4}\frac{C_n}{\mathcal{M}_n^{exp}}\right)^{\frac{1}{2n}} \tag{9}$$

with the experimental moments

$$\mathcal{M}_n^{exp} = \int ds \frac{R(s)}{s^{n+1}}\,. \tag{10}$$

The calculation of the theoretical moments C_n proceeds as follows: The diagrams are generated using `qgraf`[24]. In total there are 701 four-loop diagrams of the propagator type. Some of these diagrams are singlet diagrams, i.e. diagrams with massless cuts, and are not considered in this work. Subsequently the diagrams are expanded in the external momentum q^2 and mapped to six topologies of vacuum integrals. This is done using `q2e` and `exp` [25] in combination with MATAD [26] written in `FORM` [27]. This procedure leads to integrals with a maximum of 12 additional powers of propagators and 8 irreducible scalar products. The large number of integrals obtained in this step can be reduced to a small set of master integrals solving a large system of linear equations generated by Integration-by-Parts (IBP) identities [28]. This reduction is achieved using Laporta's algorithm [12] implemented in CRUSHER [29]. This standard method can be assisted by a special treatment of integrals containing self energies, which is described in detail in Section 3. It has to be noted that this aforementioned reduction comprises the most difficult part of the calculation. The master integrals have been calculated in [30–38]. After performing the renormalization of the quark masses and the strong coupling constant in the $\overline{\text{MS}}$ scheme the results given in Section 4 are obtained.

3 Reduction technique for integrals with internal self energies

3.1 Algorithm

The required CPU time for the reduction of Feynman integrals of a given topology to master integrals using Laporta's algorithm strongly depends on

the powers of the propagators and scalar products. For a fixed depth of a Taylor expansion in an external momentum of a Feynman amplitude the maximal number of propagator powers will appear on those integrals which contain the maximal number of self energy insertions. In the case of 4-loop tadpoles we have at most 3 self energy subgraphs which lead to a sum of propagator powers raised by 2 compared to the generic case without self energies. Such integrals are thus particularly difficult for Laporta's algorithm. On the other hand the presence of self energy insertions can be exploited to perform the reduction to master integrals in two less expensive steps, first, the reduction of the self energy subgraphs and, second, the reduction of the remaining integral. In the second step Intgration-by-Parts relations are constructed in which the self energy master integrals are treated as objects depending only on their external momentum q. In the following the procedure is illustrated for an arbitrary integral which contains a self energy insertion:

T = 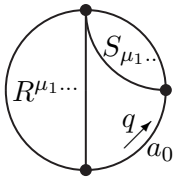

$= \int d^dq R^{\mu_1\ldots\mu_n}(q,m) S_{\mu_1\ldots\mu_n}(q,m) P^{a_0}_{m_0}(q^2)\ , \quad (11)$

where $S_{\mu_1\ldots\mu_n}(q,m)$ is a rank n tensor self energy integral, $R^{\mu_1\ldots\mu_n}(q,m)$ is the rest graph, and $P^{a_0}_{m_0}(q^2) = (q^2 - m_0^2)^{-a_0}$ is the connecting propagator with mass m_0. All masses are assumed to be either zero or m. $S_{\mu_1\ldots\mu_n}(q,m)$ is expressed in terms of a complete set of Lorentz structures $\{\Pi^p_{\mu_1\ldots\mu_n}\}$ of rank n consisting of the momentum q and the metric $g^{\mu\nu}$, and the (scalar) self energy master integrals $S_z(q^2,m)$:

$$S_{\mu_1\ldots\mu_n}(q,m) = \sum_p \Pi^p_{\mu_1\ldots\mu_n} \sum_z c^p_z(d,q^2,m) S_z(q^2,m)\ . \quad (12)$$

The coefficients $c^p_z(d,q^2,m)$ are rational functions of the space-time dimension d, the momentum q^2, and the mass m. Inserting this decomposition into (11) gives

$$T = \int d^dq \sum_p R^{\mu_1\ldots\mu_n}(q,m) \Pi^p_{\mu_1\ldots\mu_n}(q) P^{a_0}_{m_0}(q^2) \sum_z c^p_z(d,q^2,m) S_z(q^2,m). \quad (13)$$

The rest graph tensor is contracted with the Lorentz structures to

$$R^{\mu_1\ldots\mu_n}(q,m) \Pi^p_{\mu_1\ldots\mu_n}(q) = R^p(q^2,m). \quad (14)$$

From the structure of the IBP identites we know, that the q^2 dependence of the denominators of the coefficients $c^p_z(d,q^2,m)$ factorizes into propagator-like objects $P_k(q^2,m) = (q^2 - k^2m^2)^{-1}$, where k takes values from a finite set of integers depending on the type of the self energy. Partial fractioning leads to

$$P^{a_0}_{m_0}(q^2) c^p_z(d,q^2,m) = \sum_k \sum_{r_k} \tilde{c}^{p,k,r_k}_z(d) P^{r_k}_k(q^2,m), \quad (15)$$

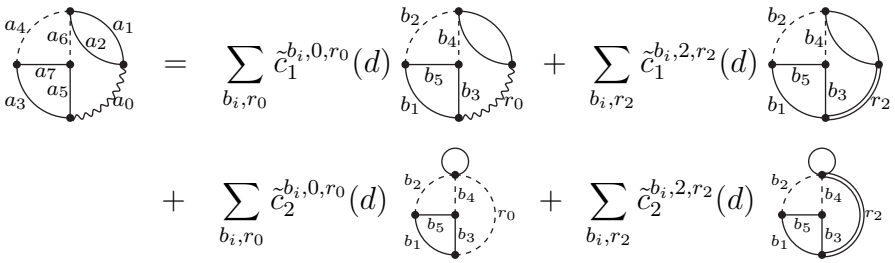

Fig. 1. The figure above shows an example of eq. (17) for a four-loop tadpole. Note that on the right hand side besides massless (dashed) lines and lines with mass m (solid) also a line with mass $2m$ (double line) appears which is not present in the initial integral. The next step would be to repeat the procedure for the two-loop self energy.

where $P_{m_0}(q^2)$ was written as $P_k(q^2, m)$ with $m_0 = km$. By convention we choose $r_k \geq 0$ for $k \neq 0$ so that the decomposition (15) is unique. After applying these transformations the integral T takes the form

$$T = \int d^d q \sum_p R^p(q^2, m) \sum_z \sum_k \sum_{r_k} \tilde{c}_z^{p,k,r_k}(d) P_k^{r_k}(q^2, m) S_z(q^2, m), \tag{16}$$

which can be written more conveniently as

$$T = \sum_k \sum_z \sum_p \sum_{r_k} \tilde{c}_z^{p,k,r_k}(d) T_z^k(\rho^p, r_k, m) \tag{17}$$

with

$$T_z^k(\rho^p, r_k, m) = \int d^d q \; R^p(q^2, m) P_k^{r_k}(q^2, m) S_z(q^2, m). \tag{18}$$

ρ^p denotes the set of propagator powers of the rest graph. That means the initial integral T is expressed as a linear combination of integrals of the type $T_z^k(\rho^p, r_k, m)$ in which the self energy insertions appear only as master integrals and all cross talking momenta between the self energy and the rest graph are removed. Figure 1 illustrates eq. (18) for a four-loop vacuum diagram.

The next step is to construct Integration-by-Parts identities for the integrals T_z^k in which the self energy insertions are treated as objects depending only on their external momenta. The identities have the form

$$\begin{aligned} 0 &= \int d^d q \, \frac{\partial}{\partial k_\mu} \ell_\mu R^p(q^2, m) P_k^{r_k}(q^2, m) S_z(q^2, m) \qquad (19) \\ &= \delta_{k\ell} \, d \, T_z^k(\rho^p, r_k, m) + \int d^d q \left[\ell_\mu \frac{\partial}{\partial k_\mu} \right]_I R^p(q^2, m) P_k^{r_k}(q^2, m) S_z(q^2, m) \\ &= \delta_{k\ell} \, d \, T_z^k(\rho^p, r_k, m) \\ &+ \int d^d q \left(\left[\ell_\mu \frac{\partial}{\partial k_\mu} \right]_I R^p(q^2, m) \right) P_k^{r_k}(q^2, m) S_z(q^2, m) \end{aligned}$$

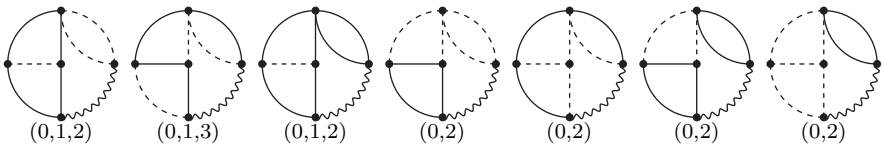

Fig. 2. All four-loop tadpoles with self energy insertions which appear in our calculation can be mapped to these seven topologies. Dotted lines are massless and solid lines carry the mass m. The wavy propagator which connects the self energies appears with the masses km where k is an element of the list below the corresponding diagram.

$$+\int d^dq R^p(q^2,m)\left(\ell_\mu\frac{\partial}{\partial k_\mu}P_k^{r_k}(q^2,m)\right)S_z(q^2,m)$$
$$+\int d^dq R^p(q^2,m)P_k^{r_k}(q^2,m)\left(\ell_\mu\frac{\partial}{\partial k_\mu}S_z(q^2,m)\right),$$

where k is a loop momentum (i. e. either q or a loop momentum of R^p) and ℓ is a loop momentum or, if present, an external momentum. The notation $\ell_\mu[\partial/\partial k_\mu]_I R^p(q^2,m)$ means that the derivative acts on the integrand of $R^p(q^2,m)$. This part and the contribution $\ell_\mu\partial/\partial k_\mu P_k^{r_k}(q^2,m)$ are treated like in traditional IBP. The difference is the treatment of $\partial/\partial k_\mu S_z(q^2,m)$ in the case $k=q$ where the derivative acts on the self energy. The derivative is explicitly performed and the resulting integrals are reduced to the self energy master integrals S_z. The coefficients appearing in this reduction require partial fractioning in q^2 again like in (15). Afterwards all terms in (19) are expressed by T_z^k and the system of equations is solved by the Laporta algorithm.

In the case of four-loop tadpoles with a one-loop self energy insertion the restgraph is a two-loop self energy. Therefore the procedure above is applied to the two-loop self energy in a second pass. The topologies which appear in our calculation are depicted in Fig. (2).

Let us add a few remarks at this point. The number of integers on which a topology T_z^k depends is given by the number of propagators of the initial topology T minus the number of propagators of the self energy subgraphs and the cross talking scalar products. In the case of four-loop tadpoles only one propagator power of initially ten (eight propagators and two irreducible scalar products) survives this procedure. Therefore the combinatorics of the IBP system for the T_z^k is much better behaved than for the initial topology. There is a price to pay for this simplification, of course. The reduction of subgraphs and the partial fractioning of propagators which carry the same momentum but different masses leads to a system of IBP relations which couples different topologies. Reducing a single propagator power from a self energy can produce two powers on an external leg, therefore in the worst case the total number of propagator powers might be doubled. If the rest graph is sufficiently simple these issues are easy to deal with. Futhermore, the tensor reduction of large powers of cross-talking scalar products will produce

huge intermediate expressions and many terms in eq. (17). These expressions simplify to the full reduction to master integrals when the solution of the IBP system (19) is inserted. The procedure was implemented in a `Mathematica` program.

3.2 Implementation in `FIRE`

Additionally to the stand-alone implementation mentioned above, for one-loop self energy insertions the procedure was also realized with the help of the `FIRE` algorithm [39].

Instead of the tensor reduction (12) the so-called *region-bases* feature of `FIRE` is used. The tensor structure arises from scalar products of loop-momenta between the self energy and the rest graph. The `SBases` program [40] can construct a basis of recursion relations to reduce the power of these cross-talking scalar products to zero without caring about the rest of the intgeral. Such a basis is called a *region-basis*. In the second step the scalar self energy integrals are reduced to master integrals. This can either be done by a region-basis, or with the help of precalculated reduction tables in combination with the *Rules* feature of `FIRE`.

In the case of one-loop self energies with one mass (either massive-massive or massive-massless) two master integrals appear, the massive tadpole and the self energy with both propagator powers equal to one. Integrals which contain the tadpole are treated like usual integrals with one loop less than the initial integral, because the tadpole factorizes from the rest of the intgeral. The treatment of integrals with the self energy master insertion is a bit more complicated. One has to introduce a new object in Feynman diagrams. We call this a *heavy dot* which can be either present (integral has a self energy master insertion), or not (integral has a tadpole insertion) and is therefore represented by an index which is either zero or one.

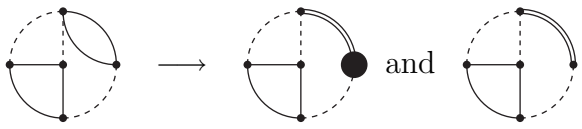

Note that we also have to introduce additional lines which carry masses depending on the self energy type. The massive-massive self energy needs a massless and a double-massive line, the massive-massless self energy needs a massless and a usual massive line that is external with respect to the self energy (one of these is naturally present in the initial diagram). These lines are needed to absorb the momentum dependence of the coefficients from the reduction of the self energies to master integrals. The partial fractioning of these two lines is done by a recursion relation which is added to the region ba-

sis. The IPBs for the remaining integrals are constructed as in eq. (19) where the creation or destruction of a heavy dot is done by a shift operator for the corresponding index, just like for usual propagators. The reduction procedure aims on reducing the heavy dot index to zero if possible. The `FIRE` program has a setting allowing to use the heavy dots and can create SBases for integrals with heavy dots present. However, the IBP generator coming with `FIRE` at the moment is not able to construct such IBP relation. As it has been explained above, the procedure can be repeated if a second self energy is present and one can again consider a region-basis corresponding to the second self energy subdiagram, insert rules reducing it to masters and finally result in a problem with two heavy dots.

3.3 Top level reduction

Although the approach from above is not applicable to general Feynman integrals, in combination with `FIRE` for the top level reduction it can be used for the calculation of arbitrary integrals. In the highest sectors the SBases are used to reduce the integrals until enough lines are contracted so that only integrals with internal self energies are left. From experience we know that the SBases algorithm often fails in sectors where self energy insertions are present. At this point a program that implements the above procedure is plugged in with the rules framework of `FIRE` to automatically finish the reduction. This way we do not need SBases for the lower sectors for which in some cases we could not find a basis. In combination with the top level reduction single integrals can be calculated if needed or for checks. However, at present this approach is not suited for large scale calculations. The self energy formalism itself is very efficient and can be used to significantly reduce the effort to invest in Laporta algorithm.

4 Results

In this Section we present the numerical values of all moments known at $\mathcal{O}(\alpha_s^3)$ for the different currents. The full analytical expressions of the new four-loop contributions can be found in Appendix A. We present results up to the third moment for the scalar, vector and axial-vector correlators. In the case of the pseudo-scalar current the n-th moment is related to the $(n-1)$-th moment of the longitudinal part of the axial-vector current through the Ward identity

$$q^2\Pi_L^a(q^2) = 4m^2(\Pi^p(q^2) - q^2(\partial\Pi^p(q^2)/\partial q^2)|_{q^2=0})\,. \tag{20}$$

This allows to obtain the fourth moment of the pseudo-scalar current. The numerical values are obtained setting the renormalization scale $\mu = m$ and using

the $\overline{\rm MS}$ scheme for the renormalization of the quark masses. We explicitely keep the dependence on the number of light quarks n_l and set the number of heavy quarks $n_h = 1$. For completeness we give the numerical values for all terms in the perturbative series in α_s up to $\mathcal{O}(\alpha_s^3)$.

$$\begin{aligned}
C_1^v =& 1.06666 + 2.55473\frac{\alpha_s}{\pi} + (0.50988 + 0.66227 n_l)\left(\frac{\alpha_s}{\pi}\right)^2 \\
&+ (1.87882 - 2.79472 n_l + 0.09610 n_l^2)\left(\frac{\alpha_s}{\pi}\right)^3, \\
C_2^v =& 0.45714 + 1.10955\frac{\alpha_s}{\pi} + (1.41227 + 0.45491 n_l)\left(\frac{\alpha_s}{\pi}\right)^2 \\
&+ (-6.23488 + 0.96156 n_l - 0.01594 n_l^2)\left(\frac{\alpha_s}{\pi}\right)^3, \\
C_3^v =& 0.27089 + 0.51939\frac{\alpha_s}{\pi} + (0.35222 + 0.42886 n_l)\left(\frac{\alpha_s}{\pi}\right)^2 \\
&+ (-8.30971 + 1.94219 n_l - 0.03959 n_l^2)\left(\frac{\alpha_s}{\pi}\right)^3
\end{aligned}$$

$$\begin{aligned}
C_1^a =& 0.53333 + 0.84609\frac{\alpha_s}{\pi} + (-2.34665 + 0.41316 n_l)\left(\frac{\alpha_s}{\pi}\right)^2 \\
&+ (-1.16280 - 0.56583 n_l + 0.04784 n_l^2)\left(\frac{\alpha_s}{\pi}\right)^3, \\
C_2^a =& 0.15238 + 0.14165\frac{\alpha_s}{\pi} + (-0.83002 + 0.19218 n_l)\left(\frac{\alpha_s}{\pi}\right)^2 \\
&+ (-6.95414 + 1.11092 n_l - 0.02049 n_l^2)\left(\frac{\alpha_s}{\pi}\right)^3, \\
C_3^a =& 0.06772 - 0.01276\frac{\alpha_s}{\pi} + (-0.67592 + 0.13562 n_l)\left(\frac{\alpha_s}{\pi}\right)^2 \\
&+ (-5.36382 + 0.98605 n_l - 0.02233 n_l^2)\left(\frac{\alpha_s}{\pi}\right)^3,
\end{aligned}$$

$$\begin{aligned}
C_1^s =& 0.8 + 0.60246\frac{\alpha_s}{\pi} + (-9.50321 + 0.58765 n_l)\left(\frac{\alpha_s}{\pi}\right)^2 \\
&+ (2.36044 - 3.31076 n_l + 0.23981 n_l^2)\left(\frac{\alpha_s}{\pi}\right)^3, \\
C_2^s =& 0.22857 + 0.42582\frac{\alpha_s}{\pi} + (-1.44346 + 0.23664 n_l)\left(\frac{\alpha_s}{\pi}\right)^2 \\
&+ (-16.84601 + 1.28345 n_l + 0.00398 n_l^2)\left(\frac{\alpha_s}{\pi}\right)^3, \\
C_3^s =& 0.10158 + 0.15355\frac{\alpha_s}{\pi} + (-0.60909 + 0.15633 n_l)\left(\frac{\alpha_s}{\pi}\right)^2
\end{aligned}$$

$$+ (-10.40154 + 1.32090 n_l - 0.01802 n_l^2) \left(\frac{\alpha_s}{\pi}\right)^3,$$

$$\begin{aligned}
C_1^p =& 1.33333 + 3.11111 \frac{\alpha_s}{\pi} + (-1.73650 + 0.61728 n_l) \left(\frac{\alpha_s}{\pi}\right)^2 \\
&+ (21.34792 - 8.66336 n_l + 0.37997 n_l^2) \left(\frac{\alpha_s}{\pi}\right)^3 \\
C_2^p =& 0.53333 + 2.06419 \frac{\alpha_s}{\pi} + (6.36704 + 0.28971 n_l) \left(\frac{\alpha_s}{\pi}\right)^2 \\
&+ (10.92473 - 1.49687 n_l + 0.07020 n_l^2) \left(\frac{\alpha_s}{\pi}\right)^3, \\
C_3^p =& 0.30476 + 1.21171 \frac{\alpha_s}{\pi} + (5.19573 + 0.26782 n_l) \left(\frac{\alpha_s}{\pi}\right)^2 \\
&+ (13.96839 + 0.15741 n_l + 0.01535 n_l^2) \left(\frac{\alpha_s}{\pi}\right)^3, \\
C_4^p =& 0.20317 + 0.71275 \frac{\alpha_s}{\pi} + (3.40816 + 0.28627 n_l) \left(\frac{\alpha_s}{\pi}\right)^2 \\
&+ (10.20740 + 1.06763 n_l - 0.00916 n_l^2) \left(\frac{\alpha_s}{\pi}\right)^3,
\end{aligned}$$

We find full analytical and numerical agreement with all previously known results, which means C_1^v from Refs [18,19] and C_1^δ and C_2^p from Ref. [23].

In [6] the value of the third moment of the vector current has been predicted $C_3^v = -3.279 \pm 0.573, -1.457 \pm 0.579$ for $n_l = 3, 4$, respectively. The calculated values -2.839 and -1.174 are within these error bound. They also lie well within the estimates of [4].

5 Applications

One of the main applications of the low-energy moments of the vacuum polarization function is the determination of the charm- and bottom-quark masses using sum rules. As can be seen from Eq. (9) the masses can be extracted from the experimental measurement of the R-ratio in the threshold region of open charm or bottom production. This relation has been exploited in [4] where only the first moment of the vector correlator was used. Recently, new data from the Babar collaboration was published for the region around the $b\bar{b}$ threshold [41]. Since a full analysis of this new data is beyond the scope of this paper, we only quote the results from [42], where besides the new Babar data also all moments presented in this work were included. It turns out that

moment	$m_c(3\text{ GeV})$[GeV] Ref. [5]	$m_c(3\text{ GeV})$[GeV]
2	0.986(11)	0.986(11)
3	0.986(10)	0.986(10)
4	0.973(19)	0.981(13)
5	0.969(23)	0.975(17)

Table 1
Update of the results from Table II given in [5] for m_c extracted using the pseudo-scalar correlator. The value of the fifth moment was taken from Ref. [7].

our new results lead to a reduction of the theoretical uncertainty by about 6 – 10 MeV while the mean values extracted using different moments get only shifted by about 2 – 4 MeV. The values of the quark masses obtained from the different moments are in good agreement which demonstrates the consistency of the method. The final values for the charm and bottom quark read

$$m_c(3\text{GeV}) = 0.986(13)\text{GeV}\,, \tag{21}$$
$$m_b(m_b) = 4.163(16)\text{GeV}\,. \tag{22}$$

In the case of the charm quark the experimental data can be replaced by lattice "data", i.e. data obtained from the calculation of appropriate correlators on the lattice. This has recently been done by the HPQCD collaboration in Ref. [5]. They found that in practice the pseudo-scalar correlator is best suited for these calculations, but also the other currents can be used with less accuracy. In Table 1 we give an update of the results in [5] where our result for the third moment of the pseudo-scalar correlator was already used prior to this publication. The values of the charm-quark mass extracted using different moments are in very good agreement with each other and the results from analyses using experimental data as input.

Lattice calculations can also be used to determine the value of the strong coupling constant as explained in detail in [5]. Again the pseudo-scalar correlator is best suited and in Table 2 we give an update of the numbers presented in [5]. The values from different moments are again in very good agreement with each other and competitive with the world average for $\alpha_s(M_Z) = 0.1176(20)$

6 Conclusion

We calculated the second and third low-energy moment of the heavy quark correlator for vector, scalar and axial-vector currents and derived the fourth moment of the pseudo-scalar correlator. To this end we discussed new methods based on Sbases and reduction of internal self-energies for the reduction of

moment	$\alpha_s(3\,\mathrm{GeV})$ Ref. [5]	$\alpha_s(3\,\mathrm{GeV})$	$\alpha_s(M_Z)$
1	0.252(6)	0.252(6)	0.1177(12)
2/3	0.249(6)	0.249(6)	0.1170(13)
3/4	0.224(31)	0.237(11)	0.1145(25)
4/5	0.241(30)	0.236(19)	0.1143(44)

Table 2
Update of the results for α_s from Table II given in [5]. The values of α_s are extracted using the indicated ratios of moments. The value of the fifth moment was taken from Ref. [7].

scalar integrals to masters. Furthermore we give an update of the results for the quark masses and α_s obtained in previous publications. The new results presented reduce the uncertainty on the quark masses by about 6 – 10 MeV while the central values are only shifted by about 2 – 4 MeV. This demonstrates the validity of the method used for the mass determination. Furthermore the new results can be used to improve the reconstruction of $\Pi(q^2)$ over the whole energy range using Padé approximation.

Acknowledgements

We thank K. G. Chetyrkin and J. H. Kühn for helpful discussions and M. Steinhauser and C. Sturm for providing the update of the lattice results. This work was supported by the Deutsche Forschungsgemeinschaft through the SFB/TR-9 "Computational Particle Physics". Ph. M. was supported by the Graduiertenkolleg "Hochenergiephysik und Teilchenastrophysik". A. M. thanks the Landesgraduiertenförderung for support. The work of A. S. was supported in part by the Russian Foundation for Basic Research through grant 08-02-01451.

A Analytical Results

In this Appendix we list the analytical results for the different currents where we used the abbreviations

$$\begin{aligned} c_4 =& 24a_4 + \log^4(2) - 6\zeta_2 \log^2(2)\,, \\ a_n =& \mathrm{Li}_n(\tfrac{1}{2}) = \sum_{k=1}^{\infty} \frac{1}{2^k k^n}\,, \\ \zeta_n =& \sum_{k=1}^{\infty} \frac{1}{k^n}\,. \end{aligned} \tag{A.1}$$

The results are split according to the colour structures defined in Eq. (6) and use the $\overline{\rm MS}$-scheme for the renormalization of the quark masses.

The results of this calculation can be downloaded in computer readable form from
`http://www-ttp.particle.uni-karlsruhe.de/Progdata/ttp09/ttp09-18/`.

A.1 Second moments

A.1.1 Vector current

$$
\begin{aligned}
C^{(3),v}_{ll,2} =& \frac{15441973}{19136250} - \frac{32}{45}\zeta_3,\\
C^{(3),v}_{hh,2} =& \frac{1842464707}{646652160} - \frac{2744471}{1064448}\zeta_3,\\
C^{(3),v}_{lh,2} =& \frac{95040709}{62705664} - \frac{2029}{41472}c_4 + \frac{99421}{55296}\zeta_4 - \frac{12159109}{4644864}\zeta_3,\\
C^{(3),v}_{lNA,2} =& -\frac{22559166733}{16796160000} - \frac{520999}{4354560}c_4 + \frac{167529079}{5806080}\zeta_4 - \frac{309132631}{12902400}\zeta_3,\\
C^{(3),v}_{lA,2} =& \frac{357543003871}{11757312000} + \frac{520999}{2177280}c_4 + \frac{598455689}{2903040}\zeta_4 - \frac{36896356307}{174182400}\zeta_3,\\
C^{(3),v}_{hNA,2} =& -\frac{20427854209619}{5649153269760} - \frac{31595849}{11612160}c_4 + \frac{968787977}{15482880}\zeta_4 + \frac{362}{63}\zeta_5\\
& - \frac{29638030087837}{697426329600}\zeta_3,\\
C^{(3),v}_{hA,2} =& -\frac{37320009196157}{271593907200} - \frac{130387543}{2177280}c_4 + \frac{2218910663}{1451520}\zeta_4\\
& - \frac{5811074101069}{6706022400}\zeta_3,\\
C^{(3),v}_{n^0_f,2} =& \frac{64985074258811347}{353072079360000} - \frac{1662518706713}{21016195200}c_4 - \frac{26401638588211}{28021593600}\zeta_4\\
& - \frac{164928917}{270270}\zeta_5 - \frac{2900811008}{3648645}a_5 - \frac{1684950406}{3648645}\log(2)\zeta_4\\
& - \frac{725202752}{10945935}\log^3(2)\zeta_2 + \frac{362601376}{54729675}\log^5(2)\\
& + \frac{112680551036302633}{47076277248000}\zeta_3\,.
\end{aligned}
$$

A.1.2 Scalar current

$$
C^{(3),s}_{n_f,2} = \frac{381690470169079}{467026560000} + \frac{66906848}{1216215}a_5 + \frac{402167880157}{28021593600}c_4
$$

$$
\begin{aligned}
&- \frac{8363356}{18243225}\log^5(2) + \frac{16726712}{3648645}\log^3(2)\zeta_2 - \frac{87227759}{1216215}\log(2)\zeta_4 \\
&- \frac{1075951565336201}{560431872000}\zeta_3 + \frac{3294508921817}{5337446400}\zeta_4 + \frac{480273679}{694980}\zeta_5, \\
C^{(3),s}_{hN,2} =& - \frac{355706449933319}{37661021798400} - \frac{4135403}{2150400}c_4 - \frac{857749280491}{37196070912}\zeta_3 \\
&+ \frac{83367701}{1720320}\zeta_4 - \frac{25}{21}\zeta_5, \\
C^{(3),s}_{lN,2} =& - \frac{102230727187}{19595520000} - \frac{1121}{48384}c_4 + \frac{986734811}{58060800}\zeta_3 - \frac{4419371}{322560}\zeta_4, \\
C^{(3),s}_{hA,2} =& \frac{589278012260869}{2353813862400} + \frac{21022661}{181440}c_4 + \frac{98124313871713}{58118860800}\zeta_3, \\
&- \frac{357046549}{120960}\zeta_4 \\
C^{(3),s}_{lA,2} =& - \frac{12729644591}{279936000} + \frac{1121}{24192}c_4 + \frac{1192980407}{9676800}\zeta_3 - \frac{5073991}{53760}\zeta_4, \\
C^{(3),s}_{lh,2} =& \frac{64429199}{41803776} - \frac{1301}{27648}c_4 - \frac{37067899}{15482880}\zeta_3 + \frac{63749}{36864}\zeta_4, \\
C^{(3),s}_{hh,2} =& \frac{34805101}{6735960} - \frac{101467}{23760}\zeta_3, \\
C^{(3),s}_{ll,2} =& \frac{1439317}{6378750} - \frac{8}{45}\zeta_3\,.
\end{aligned}
$$

A.1.3 Axial-vector current

$$
\begin{aligned}
C^{(3),a}_{n_f,2} =& \frac{217627345572539363}{29957630976000} - \frac{22929814528}{18243225}a_5 + \frac{48366697030607}{367783416000}c_4 \\
&+ \frac{2866226816}{273648375}\log^5(2) - \frac{5732453632}{54729675}\log^3(2)\zeta_2 \\
&- \frac{5480723618}{2606175}\log(2)\zeta_4 - \frac{19481983397047414063}{3295339407360000}\zeta_3 \\
&- \frac{3999530651550337}{980755776000}\zeta_4 + \frac{64302085207}{12162150}\zeta_5, \\
C^{(3),a}_{hN,2} =& - \frac{58553635489580981}{3954407288832000} - \frac{5032917199}{3048192000}c_4 - \frac{289668262443149}{19527937228800}\zeta_3 \\
&+ \frac{40203350213}{812851200}\zeta_4 - \frac{382}{45}\zeta_5, \\
C^{(3),a}_{lN,2} =& - \frac{414223585133}{33592320000} - \frac{2041307}{43545600}c_4 + \frac{43700406067}{696729600}\zeta_3 - \frac{95269223}{1658880}\zeta_4, \\
C^{(3),a}_{hA,2} =& \frac{30093199294856077}{35307207936000} + \frac{707672969}{1814400}c_4 + \frac{1650262562573011}{290594304000}\zeta_3 \\
&- \frac{1718278879}{172800}\zeta_4, \\
C^{(3),a}_{lA,2} =& - \frac{4855444846081}{23514624000} + \frac{2041307}{21772800}c_4 + \frac{30349640587}{49766400}\zeta_3 - \frac{2828510767}{5806080}\zeta_4,
\end{aligned}
$$

$$
\begin{aligned}
C_{lh,2}^{(3),a} =& \frac{809030351}{627056640} - \frac{2797}{82944}c_4 - \frac{92264351}{46448640}\zeta_3 + \frac{137053}{110592}\zeta_4, \\
C_{hh,2}^{(3),a} =& \frac{1173822473}{323326080} - \frac{24710027}{7983360}\zeta_3, \\
C_{ll,2}^{(3),a} =& \frac{4275743}{19136250} - \frac{32}{135}\zeta_3\,.
\end{aligned}
$$

A.2 Third moments

A.2.1 Vector current

$$
\begin{aligned}
C_{ll,3}^{(3),v} =& \frac{31556642272}{49228003125} - \frac{256}{405}\zeta_3, \\
C_{hh,3}^{(3),v} =& \frac{56877138427}{12609717120} - \frac{6184964549}{1556755200}\zeta_3, \\
C_{lh,3}^{(3),v} =& \frac{60361465477}{29393280000} - \frac{1765}{31104}c_4 + \frac{86485}{41472}\zeta_4 - \frac{57669161}{17418240}\zeta_3, \\
C_{lNA,3}^{(3),v} =& -\frac{1475149211788337}{6452412825600000} - \frac{8529817}{77414400}c_4 + \frac{1510937903}{14745600}\zeta_4 \\
& - \frac{561258009401}{6193152000}\zeta_3, \\
C_{lA,3}^{(3),v} =& \frac{983812946922223}{4389396480000} + \frac{8529817}{38707200}c_4 + \frac{21972351293}{17203200}\zeta_4 \\
& - \frac{28995540810097}{21676032000}\zeta_3, \\
C_{hNA,3}^{(3),v} =& -\frac{454880458419083629}{5854170457175040000} - \frac{7110196837}{1117670400}c_4 + \frac{1068488091383}{7451136000}\zeta_4 \\
& + \frac{4448}{315}\zeta_5 - \frac{43875740175477222611}{433642256087040000}\zeta_3, \\
C_{hA,3}^{(3),v} =& -\frac{2327115263308753}{2489610816000} - \frac{16870125343}{39916800}c_4 + \frac{286864384271}{26611200}\zeta_4 \\
& - \frac{377837317054807}{61471872000}\zeta_3, \\
C_{n_f^0,3}^{(3),v} =& \frac{80110016771563030091836 63}{12705510619017216000 00} - \frac{16091704629458603}{45731240755200}c_4 \\
& - \frac{1505000915688143609}{304874938368000}\zeta_4 - \frac{1781851011826}{310134825}\zeta_5 - \frac{859399602944}{310134825}a_5 \\
& - \frac{38830116184}{44304975}\log(2)\zeta_4 - \frac{214849900736}{930404475}\log^3(2)\zeta_2 \\
& + \frac{107424950368}{4652022375}\log(2)^5 + \frac{1061162538194750079871}{128047474114560000}\zeta_3\,.
\end{aligned}
$$

A.2.2 Scalar current

$$
\begin{aligned}
C^{(3),s}_{ll,3} =& \frac{2229649183}{16409334375} - \frac{64}{405}\zeta_3,\\
C^{(3),s}_{hh,3} =& \frac{82738947097}{12009254400} - \frac{11973270941}{2075673600}\zeta_3,\\
C^{(3),s}_{lh,3} =& \frac{1047601560409}{627056640000} - \frac{139777}{3317760}c_4 + \frac{6849073}{4423680}\zeta_4 - \frac{4641507553}{1857945600}\zeta_3,\\
C^{(3),s}_{lNA,3} =& -\frac{22504447164310009}{1075402137600000} - \frac{2832217}{116121600}c_4 - \frac{288902173}{4423680}\zeta_4\\
&+ \frac{142693634059}{1857945600}\zeta_3,\\
C^{(3),s}_{lA,3} =& -\frac{296129104756579}{1024192512000} + \frac{2832217}{58060800}c_4 - \frac{51185293321}{77414400}\zeta_4\\
&+ \frac{1811694475921}{2167603200}\zeta_3,\\
C^{(3),s}_{hNA,3} =& -\frac{549859189388336126083}{31222242438266880000} - \frac{270366644899}{89413632000}c_4 + \frac{1953161743091}{23843635200}\zeta_4\\
&- \frac{1888}{315}\zeta_5 - \frac{16019821402882223177}{462551739826176000}\zeta_3,\\
C^{(3),s}_{hA,3} =& \frac{1248837940639034917}{838406080512000} + \frac{108697503829}{159667200}c_4 - \frac{263931412979}{15206400}\zeta_4\\
&+ \frac{4308361964639349413}{434729078784000}\zeta_3,\\
C^{(3),s}_{n^0_f,3} =& \frac{1831719443479347906961831}{211758510316953600000} + \frac{23476362679129111}{266765571072000}c_4\\
&- \frac{227245780513489691}{71137485619200}\zeta_4 + \frac{550981545544}{103378275}\zeta_5 - \frac{31233089024}{103378275}a_5\\
&- \frac{132939852688}{103378275}\log(2)\zeta_4 - \frac{7808272256}{310134825}\log^3(2)\zeta_2\\
&+ \frac{3904136128}{1550674125}\log(2)^5 - \frac{6840706109244803149}{798870159360000}\zeta_3\,.
\end{aligned}
$$

A.2.3 Axial-vector current

$$
\begin{aligned}
C^{(3),a}_{ll,3} =& \frac{6052378456}{49228003125} - \frac{64}{405}\zeta_3,\\
C^{(3),a}_{hh,3} =& \frac{599209514131}{126097171200} - \frac{12494549257}{3113510400}\zeta_3,\\
C^{(3),a}_{lh,3} =& \frac{4962625369889}{3762339840000} - \frac{630217}{19906560}c_4 + \frac{30880633}{26542080}\zeta_4 - \frac{21887209193}{11147673600}\zeta_3,\\
C^{(3),a}_{lNA,3} =& -\frac{41502247972857197}{955913011200000} - \frac{254785409}{8360755200}c_4 - \frac{2632884019279}{11147673600}\zeta_4
\end{aligned}
$$

$$
\begin{aligned}
&+\frac{55622383674929}{222953472000}\zeta_3,\\
C^{(3),a}_{lA,3} =&-\frac{407919130830390283}{368709304320000}+\frac{254785409}{4180377600}c_4-\frac{17645944577969}{5573836800}\zeta_4\\
&+\frac{2942092239074473}{780337152000}\zeta_3,\\
C^{(3),a}_{hNA,3} =&-\frac{9291278450921361191597}{266210698684170240000}-\frac{131718995983}{1609445376000}c_4\\
&+\frac{12854292041443}{429185433600}\zeta_4-\frac{9376}{405}\zeta_5+\frac{29030831574992389907}{1314620734242816000}\zeta_3,\\
C^{(3),a}_{hA,3} =&\frac{167314115446749909343}{35213055381504000}+\frac{6229030586993}{2874009600}c_4-\frac{15127004909623}{273715200}\zeta_4\\
&+\frac{49375038643781532767}{1565024683622400}\zeta_3,\\
C^{(3),a}_{n^0_f,3} =&\frac{12292520605765834001572294 37}{22869919114230988800000}+\frac{26069736016065697819}{28810681675776000}c_4\\
&-\frac{84934038473664674083}{1536569689374720}\zeta_4+\frac{29147971741346}{930404475}\zeta_5\\
&-\frac{6290348482816}{930404475}a_5-\frac{11153783461592}{930404475}\log(2)\zeta_4\\
&-\frac{1572587120704}{2791213425}\log^3(2)\zeta_2+\frac{786293560352}{13956067125}\log(2)^5\\
&-\frac{186473363797973441853 71}{1075598782562304000}\zeta_3\,.
\end{aligned}
$$

A.2.4 Pseudo-scalar current

$$
\begin{aligned}
C^{(3),p}_{ll,3} =&\frac{5893303}{9568125}-\frac{64}{135}\zeta_3,\\
C^{(3),p}_{hh,3} =&-\frac{26179537}{58786560}+\frac{76295}{290304}\zeta_3,\\
C^{(3),p}_{lh,3} =&\frac{103200341}{627056640}-\frac{1435}{82944}c_4+\frac{70315}{110592}\zeta_4-\frac{5574817}{9289728}\zeta_3,\\
C^{(3),p}_{lNA,3} =&\frac{102523166819}{11197440000}-\frac{259289}{4838400}c_4+\frac{3760967}{36864}\zeta_4-\frac{927288197}{9289728}\zeta_3,\\
C^{(3),p}_{lA,3} =&\frac{1867646866703}{7838208000}+\frac{259289}{2419200}c_4+\frac{184831769}{215040}\zeta_4-\frac{16109807909}{16588800}\zeta_3,\\
C^{(3),p}_{hNA,3} =&\frac{10104443767785889}{1318135762944000}-\frac{4409031071}{677376000}c_4+\frac{25692311767}{180633600}\zeta_4\\
&+\frac{368}{15}\zeta_5-\frac{248471102645509}{2169770803200}\zeta_3,\\
C^{(3),p}_{hA,3} =&-\frac{11809333374019073}{11769069312000}-\frac{1657837871}{3628800}c_4+\frac{28182137887}{2419200}\zeta_4\\
&-\frac{214584455705773}{32288256000}\zeta_3,
\end{aligned}
$$

$$
\begin{aligned}
C^{(3),p}_{n_f^0,3} =& -\frac{841507212739667387}{549223234560000} - \frac{62193803213161}{245188944000}c_4 - \frac{9141288770183}{5108103000}\zeta_4 \\
& - \frac{58401651592}{6081075}\zeta_5 + \frac{15214899712}{6081075}a_5 + \frac{3649219472}{868725}\log(2)\zeta_4 \\
& + \frac{3803724928}{18243225}\log^3(2)\zeta_2 - \frac{1901862464}{91216125}\log^5(2) \\
& + \frac{767220341123064149}{84495882240000}\zeta_3\,.
\end{aligned}
$$

A.3 Fourth Moments

A.3.1 Pseudo-scalar current

$$
\begin{aligned}
C^{(3),p}_{ll,4} =& \frac{329624056}{607753125} - \frac{64}{135}\zeta_3, \\
C^{(3),p}_{hh,4} =& \frac{1739021393}{4670265600} - \frac{52674403}{115315200}\zeta_3, \\
C^{(3),p}_{lh,4} =& \frac{6245190619}{9289728000} - \frac{18589}{737280}c_4 + \frac{910861}{983040}\zeta_4 - \frac{1587980983}{1238630400}\zeta_3, \\
C^{(3),p}_{lNA,4} =& \frac{331245076513169857}{8603217100800000} - \frac{964223}{15925248}c_4 + \frac{63056544809}{148635648}\zeta_4 \\
& - \frac{1229566890599}{2972712960}\zeta_3, \\
C^{(3),p}_{lA,4} =& \frac{1309551728160611}{910393344000} + \frac{964223}{7962624}c_4 + \frac{10470510368767}{1857945600}\zeta_4 \\
& - \frac{36245830807891}{5780275200}\zeta_3, \\
C^{(3),p}_{hNA,4} =& \frac{331240239758015836819 57}{16860010916664115200 00} - \frac{2883014289719}{107296358400}c_4 \\
& + \frac{87140698714231}{143061811200}\zeta_4 + \frac{11776}{189}\zeta_5 - \frac{3691162910334747972379}{8325931316871168000}\zeta_3, \\
C^{(3),p}_{hA,4} =& -\frac{217480554135087391943}{35213055381504000} - \frac{2695980497779}{958003200}c_4 \\
& + \frac{45831907340963}{638668800}\zeta_4 - \frac{106836033862656915617}{2608374472704000}\zeta_3, \\
C^{(3),p}_{n_f^0,4} =& \frac{160999779080808137440043699}{76233063714103296000 00} - \frac{15601462649447899319}{9603560558592000}c_4 \\
& - \frac{41651006271487731961}{12804747411456000}\zeta_4 - \frac{3679557604076}{62026965}\zeta_5 + \frac{133358649856}{8860995}a_5 \\
& + \frac{1559619599504}{62026965}\log(2)\zeta_4 + \frac{33339662464}{26582985}\log^3(2)\zeta_2 \\
& - \frac{16669831232}{132914925}\log(2)^5 + \frac{519180776457371224187}{21090172207104000}\zeta_3\,.
\end{aligned}
$$

References

[1] Shifman, M. A. and Vainshtein, A. I. and Zakharov, V. I. *Nucl. Phys.*, B147:448–518, 1979.

[2] Reinders, L. J. and Rubinstein, H. and Yazaki, S. *Phys. Rept.*, 127:1, 1985.

[3] Kühn, J. H. and Steinhauser, M. *Nucl. Phys.*, B619:588–602, 2001[Erratum-ibid. B **640** (2002) 415].

[4] Kühn, J. H. and Steinhauser, M. and Sturm, C. *Nucl. Phys.*, B778:192–215, 2007.

[5] Allison, I. *et al.* [HPQCD Collaboration], Phys. Rev. D **78** (2008) 054513 *[0805.2999 [hep-lat]]*.

[6] Hoang, A. H., Mateu, V. and Mohammad Zebarjad, S., Nucl. Phys. B **813** (2009) 349 *[0807.4173 [hep-ph]]*.

[7] Kiyo, Y., Maier, A., Maierhöfer, P., Marquard, P. arXiv:0907.2120 [hep-ph].

[8] Chetyrkin, K. G. and Kühn, J. H. and Steinhauser, M. *Phys. Lett.* B371 93, 1996.

[9] Chetyrkin, K. G., Kühn, J. H. and Steinhauser, M., Nucl. Phys. B **482** (1996) 213 *[hep-ph/9606230]*.

[10] Chetyrkin, K. G. and Kühn, J. H. and Steinhauser, M. *Nucl. Phys.*, B505:40–64, 1997.

[11] Broadhurst, D. J., Z. Phys. C **54** (1992) 599.

[12] Laporta, S. *Int. J. Mod. Phys.*, A15:5087–5159, 2000.

[13] Remiddi, E., Nuovo Cim. A **110** (1997) 1435 *[hep-th/9711188]*.

[14] Caffo, M., Czyz, H., Laporta, S. and Remiddi, E., Nuovo Cim. A **111** (1998) 365 *[hep-th/9805118]*.

[15] Kotikov, A. V., Phys. Lett. B **254** (1991) 158.

[16] Boughezal, R. and Czakon, M. and Schutzmeier, T. *Nucl. Phys. Proc. Suppl.*, 160:160–164, 2006.

[17] Maier, A. and Maierhöfer, P. and Marquard, P. *Nucl. Phys.*, B797:218–242, 2008.

[18] Chetyrkin, K. G. and Kühn, J. H. and Sturm, C. *Eur. Phys. J.*, C48:107–110, 2006.

[19] Boughezal, R. and Czakon, M. and Schutzmeier, T. *Phys. Rev.*, D74:074006, 2006.

[20] Maier, A., Maierhöfer, P. and Marquard, P., Phys. Lett. B **669** (2008) 88 *[0806.3405 [hep-ph]]*.

[21] Czakon, M. and Schutzmeier, T., JHEP **0807** (2008) 001 *[0712.2762 [hep-ph]]*.

[22] Grozin, A. G. and Sturm, C. *Eur. Phys. J.*, C40:157, 2005.

[23] Sturm, C., JHEP **0809**, 075 (2008) *[0805.3358 [hep-ph]]*.

[24] Nogueira, P. *J. Comput. Phys.*, 105:279–289, 1993.

[25] Harlander, R. and Seidensticker, T. and Steinhauser, M. Phys. Lett. B **426** (1998) 125 *[hep-ph/9712228]*; Seidensticker, T. *[hep-ph/9905298]*.

[26] Steinhauser, M. *Comput. Phys. Commun.*, 134:335, 2001.

[27] Vermaseren, J. A. M. *[math-ph/0010025]*, 2000.

[28] Chetyrkin, K. G. and Tkachov, F. V. *Nucl. Phys.*, B192:159–204, 1981.

[29] Marquard, P. and Seidel, D. unpublished.

[30] Chetyrkin, K. G., Faisst, M., Sturm, C. and Tentyukov, M., Nucl. Phys. B **742** (2006) 208 *[hep-ph/0601165]*.

[31] Schröder, Y. and Steinhauser, M., JHEP **0601** (2006) 051 *[hep-ph/0512058]*.

[32] Laporta, S. *Phys. Lett.*, B549:115, 2002.

[33] Chetyrkin, K. G. and Kühn, J. H. and Mastrolia, P. and Sturm, C. *Eur. Phys. J.*, C40:361, 2005.

[34] Kniehl, B. A. and Kotikov, A. V. *Phys. Lett.*, B638:531, 2006.

[35] Schröder, Y. and Steinhauser, M. *Phys. Lett.*, B622:124, 2005.

[36] Bejdakic, E. and Schröder, Y. *Nucl. Phys. Proc. Suppl.*, 160:155, 2006.

[37] Kniehl, B. A. and Kotikov, A. V. *Phys. Lett.*, B642:68, 2006.

[38] Kniehl, B. A. and Kotikov, A. V. and Onishchenko, A. I. and Veretin, O. L. *Phys. Rev. Lett.*, 97:042001, 2006.

[39] Smirnov, A. V., JHEP **0810**, 107 (2008) *[0807.3243 [hep-ph]]*.

[40] Smirnov, A. V. JHEP **0604** (2006) 026 *[hep-ph/0602078]*.

[41] Aubert, B. *et al.* [BABAR Collaboration], Phys. Rev. Lett. **102** (2009) 012001 *[0809.4120 [hep-ex]]*.

[42] Chetyrkin, K. G. et al. arXiv:0907.2110 [hep/ph].